

# Deposition of mass-selected ions in neon matrices: $\text{CS}_2^+$ and $\text{C}_6\text{F}_6^+$

Martin Lorenz and Vladimir E. Bondybey

*Institut für Physikalische und Theoretische Chemie der Technische Universität München,  
Lichtenbergstraße 4, 85747 Garching, Germany  
E-mail: bondybey@ch.tum.de*

Received May 15, 2000

Infrared, visible absorption as well as laser induced fluorescence (LIF) and excitation spectra are obtained for several simple cations deposited from a mass selected ion beam. In the present preliminary study we demonstrate the successful and clean mass selection by presenting spectra of samples obtained by depositing the isotopic  $^{34}\text{S}^{12}\text{C}^{32}\text{S}^+$  ion in natural isotopic abundance, and analysing its spectrum. Spectra of  $\text{C}_6\text{F}_6^+$  deposited from a 20 eV ion beam exhibit quite different inhomogeneous line profiles, suggesting that even the relatively low kinetic energy results in considerable damage of the solid. Analysis of the spectra indicates that the Jahn–Teller distorted vibrational structure in the doubly degenerate ground state of  $\text{C}_6\text{F}_6^+$  is strongly perturbed in the newly formed sites, which are presumably of lower symmetry. A 33–46  $\text{cm}^{-1}$  splitting of the origin and other totally symmetric bands in emission is tentatively attributed to the spin-orbit splitting in the  $^2E_{1g}$  ground state.

PACS: 33.15.Ta, 33.20.Ea, 33.20.Kf, **33.50.-j**, **39.10.+j**, **71.70.-d**

## 1. Introduction

One of the major aims of the matrix isolation technique was the preparation, stabilization, and spectroscopic characterization of radicals, ions, clusters and similar highly reactive, transient species [1,2]. While there are many methods for generating these reaction intermediates and transients, most of them share the same shortcoming, in that the species of interest are not prepared in pure form, but in a more or less complex mixture with a variety of other species. Also since the early days, an obvious solution to this problem was frequently considered: isolating the desired ions or molecules by means of mass selection. While conceptually it appears simple, implementation of this method proved for a whole variety of reasons to be quite elusive [3,4].

In the first place, only for relatively few species it is easy to generate ion beams of enough intensity to accumulate a sufficient concentration for their spectroscopic characterization. Another difficulty lies in the fact that in order to mass select the ions, they typically have to be accelerated to rather high energies, and to slow them down sufficiently for successful deposition is not a trivial task. Even if

their energy can be reduced to 10–20 eV, an ion with this energy striking the matrix whose atoms are bound by few meV will produce a lot of damage, can vaporize hundreds of atoms, penetrate deep into the matrix [5], and react with impurities and other species present in the solid [6], thus defeating the major aim of matrix isolation. A final problem lies in the space charge resulting from accumulation of the charged species in the nonconducting rare gas matrix [3]. This may result in stray electric fields deflecting the molecular ion beam and further complicating the ion deposition.

In spite of the problems outlined above, there has been in the last decade a steady progress in this field, indicating that the problems are not insurmountable. Several different groups have now reported studies successfully depositing mass selected species, and characterizing them spectroscopically. Very recently, we have completed the construction of an apparatus for investigation of mass selected species in our laboratory, and succeeded in obtaining infrared and visible absorption, laser induced fluorescence excitation and resolved emission spectra of mass selected ions. In the present paper we will first give a very short review of the existing

approaches to mass selected matrix studies, and compare our experimental setup with those previously reported. We will then briefly present our preliminary results for individual isotopic species of the  $\text{CS}_2^+$  and  $\text{C}_6\text{F}_6^+$  cations.

## 2. Mass-selection studies in rare gas matrices

The first successful studies of mass selected species in the matrix were reported some ten years ago almost simultaneously by several groups. Rivoal and coworkers, have modified an apparatus in Lausanne originally intended for gas phase cluster studies, and interfaced it to a cryostat for matrix spectroscopy [7,8]. In the earliest experiments aimed at deposition of mass selected  $\text{Ag}_3^+$  and  $\text{Ni}_3^+$  clusters the currents were apparently too low for optical detection, but over the following few years the apparatus was steadily improved by changing the experimental parameters and source geometry [5,9]. The cluster ions were produced by means of sputtering with a 10 mA primary beam of 20 keV  $\text{Kr}^+$  ions, analyzed in a quadrupole mass filter and deposited with krypton matrix gas on a sapphire window. The ions were directed to the window with the help of an accelerating field and an electrostatic lens, and after deposition neutralized by electrons from a tungsten filament. While in the early experiments fragmentation presented some problem, after further refinements it was possible to observe the UV absorption spectra of neutral silver clusters up to  $n = 39$  [10,11].

Lindsay, one of the investigators of the above study, Lombardi, and coworkers then constructed a new apparatus at the City College of New York, employing first a Wien velocity filter in place of the quadrupole mass spectrometer. Even though this filter had the disadvantage of relatively low mass resolution, this represented no problem in studies aimed at  $\text{M}_n^+$  metal clusters, where only clusters with varying values of  $n$  have to be separated. They are using the same CORDIS ion sputter source as Rivoal, Harbich et al. Over the following years, these workers have reported series of interesting studies of the absorption and resonance Raman spectra of numerous metal dimers and small clusters, including  $\text{V}_2$  [12],  $\text{W}_2$  [13],  $\text{Ta}_2$  [14],  $\text{Hf}_2$  [15],  $\text{Re}_2$  [16],  $\text{Co}_2$  [17],  $\text{Zr}_3$  [18],  $\text{Ta}_4$  [19],  $\text{Ni}_3$  [20],  $\text{Nb}_3$  [21],  $\text{Rh}_2$  [22],  $\text{Ru}_2$  [23],  $\text{Hf}_3$  [24], and  $\text{Pt}_2$  [25].

Another apparatus for mass selected studies was developed at Michigan State by Leroi and Allison, who used a quadrupole filter from a modified residual gas analyser [26]. In their early studies they were able to reproduce LIF spectrum of the  $\text{CS}_2^+$

ion in solid argon, but only the parent carbon disulfide and diatomic CS could be detected in the infrared, an observation which the authors explained in terms of neutralization of the ion accompanied by fragmentation to  $\text{CS} + \text{S}$  [3]. These authors have more recently reported that the ion yield could be greatly enhanced by adding small quantities (0.1 %) of  $\text{CO}_2$  to the matrix gas, which then traps the electrons and suppresses the ion-electron recombination [27]. They then succeeded in recording the infrared spectra of several ions, including  $\text{CF}_3^+$  [28],  $\text{CS}_2^+$  [29], and  $\text{CO}_2^+$  [27] in solid argon and neon matrices.

A whole series of highly successful investigations of mass selected species in the matrix is due to Maier and coworkers, who used the technique to investigate numerous carbon chain species, which are of considerable importance in astrophysics and for interstellar chemistry. They generate the carbon chain molecules in a hot cathode discharge source, using suitable precursor molecules, usually acetylene or its derivatives diluted by helium or argon [4,30,31]. The accelerated ions are focussed by electrostatic lenses, and after selection in a quadrupole mass filter they are guided onto the matrix surface. The deposited mass selected species were then investigated in solid neon matrices by visible or UV absorption spectroscopy using a wave-guide absorption technique. The spectra obtained in this way for the  $\text{H-C}_k\text{-H}^+$  [32,33],  $\text{H-C}_{2n}\text{-CN}^+$ , and  $\text{NC-C}_{2n}\text{-CN}^+$  [34] ions provide information complementary to our LIF studies on the same systems [35,36]. Recently, they used an electron impact source to produce the anions of the above mentioned linear chain molecules. After characterization of the anions, an electron was photo-detached and the corresponding neutral species have been studied [37,38]. They also used sputtering of a graphite target to generate and deposit ionic  $\text{C}_n^+$  cluster species, and record their spectra. Particularly exciting are their observations and assignment of the electronic absorption spectra of neutral and anionic carbon clusters,  $\text{C}_n$  and  $\text{C}_n^-$  [39–41]. In their spectra of the anions they detected a whole series of close coincidences with frequencies of the so called diffuse interstellar bands, which provided first really solid evidence for solving the long-standing mystery of their origin [42,43].

Quite recently, Moskovits and coworkers started to use a mass-selection apparatus similar to Lindsay's setup to study transition metal clusters. In the beginning, they examined the direct synthesis of metal cluster complexes by deposition of mass-selected iron clusters with excess CO as ligand [44].

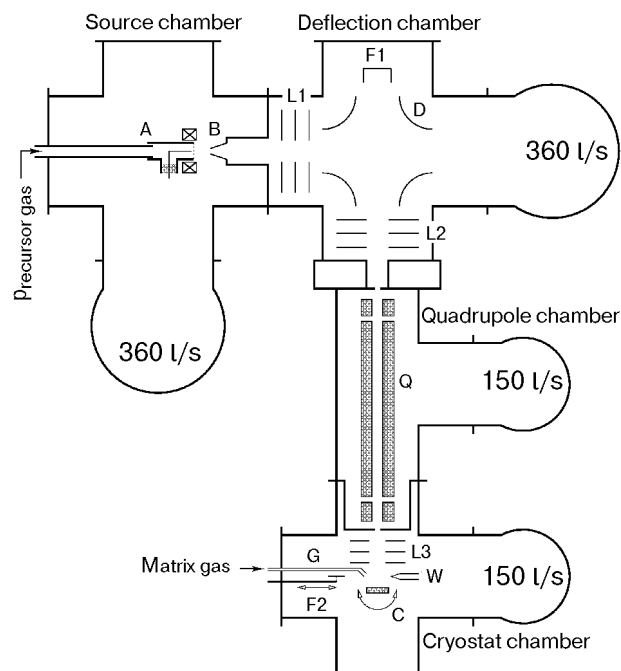


Fig. 1. Schematic of the experimental apparatus for mass selected matrix studies, with microwave discharge ion source (A), skimmer (B), first electrostatic lens (L1), deflection unit (D), first Faraday cup (F1), second lens (L2), 12mm triple stage quadrupole mass filter (Q), final lens (L3), rotatable cold surface (C), matrix gas inlet (G), movable Faraday plate (F2) and the tungsten filament (W).

Using resonance Raman spectroscopy, they were later able to characterize  $\text{Ag}_5$  [45],  $\text{Ag}_3$  and  $\text{Fe}_3$  [46] in solid argon.

### 3. Experimental

The apparatus constructed in our laboratory is similar to Maier's setup [4] – a schematic drawing is shown in Fig. 1. We have also decided to use a quadrupole mass filter, which unlike for instance time-of-flight filters, allows both pulsed and cw operation. The ion source in the present experiment was a 12 mm Swagelok T piece, with the precursor gas flowing through the colinear sections, and with 50 W of 2.45 GHz microwave power being applied to a needle electrode via the perpendicular arm. A ring shape magnet surrounding the Swagelok is used to confine the charged species produced in the discharge. The discharge products from the source held at +20 V pass through a grid and are accelerated towards a 2 mm skimmer held at -20 V. The pressure in the source chamber evacuated by a 360 l/s turbomolecular pump is  $10^{-4}$ – $10^{-2}$  mbar.

The ionic species exiting the skimmer into the deflection chamber are focused with the help of an einzel-lens L1 and deflected 90° in a quadrupole electric field. A second lens, L2, then focuses the

ions upon the entrance aperture of a quadrupole mass filter, with the undeflected neutrals being pumped by a second 360 l/s pump. A commercial triple stage HIDDEN HAL/3F quadrupole filter with 12 mm rods has a specified mass range up to 500 amu, resolution < 1 amu, and a transmission of up to 30%, when the resolution is decreased. The custom modified filter has 7 mm entrance and exit apertures, and is differentially pumped by a 150 l/s pump. The mass selected ion beam is focussed onto the matrix by means of a lens L3 and deposited simultaneously with the matrix gas, neon in the present case. The substrate, a silver coated copper plate is held at  $\approx 7$  K by a LEYBOLD RDG 580 closed-cycle refrigerator.

To maintain overall neutrality of the matrix, and avoid building up space charges and stray fields, the matrix was sprayed by electrons from a hot tungsten filament held at -100 V. We experimented with alternating the ion and electron deposition, but in the end continuous operation proved to be most efficient, with optimal results being obtained with the electron current being about five times the ion current.

In order to optimize the experiment, the ability to measure the ion current is essential. For this purpose, one Faraday cup permitting measurement of the total ion current is located in the deflection chamber. A second detector close to the cold surface allows measuring the mass selected ion current. The weak currents are amplified by a FEMTO DLPCA 100 current amplifier and digitized in the quadrupole control unit. Currents as low as 100 fA can be easily detected and we obtain mass spectra with signal : noise better than 10000 : 1. With the mass filter set to the desired mass, all the experimental parameters can be adjusted for maximum current. With our microwave discharge source we could produce for both  $\text{CS}_2^+$  and  $\text{C}_6\text{F}_6^+$  currents of mass-selected ions of up to 2 nA.

After deposition, the matrix is rotated 120° and then the matrices are characterized spectroscopically using a BRUKER IFS 120 HR Fourier transform spectrometer, equipped with beamsplitters and detectors for the 500–30000  $\text{cm}^{-1}$  spectral range. IR absorption spectra are measured with a liquid nitrogen cooled MCT (mercury-cadmium telluride) detector at a resolution of 0.06  $\text{cm}^{-1}$ , whereas all other spectra were recorded with 0.5  $\text{cm}^{-1}$  resolution. Laser excitation spectra are measured using an  $\text{Ar}^+$  laser pumped power stabilized dye laser operating with a stilbene-3 dye. The total emission of the sample is detected with a PMT (and appropriate optical filters) connected to a lock-in amplifier.

Laser induced fluorescence spectra are measured with the FT spectrometer using the same detector at a resolution of  $0.5 \text{ cm}^{-1}$ .

#### 4. Results and discussion

In our initial experiments we have investigated several ions whose matrix spectra are well known from previous studies. These ions can be durably trapped in rare gas matrices, since their electron affinity, i.e.  $10.07 \text{ eV}$  for  $\text{CS}_2^+$ , is much smaller than the ionization potential of the rare gas,  $21.56 \text{ eV}$  in the case of neon. To produce the ions, we have employed a microwave discharge through a low pressure precursor gas either pure or diluted with an inert buffer gas. In the first place, the mass spectrum of the ions emanating from the discharge was repeatedly recorded, and the source conditions were optimized for the ion of interest.

A typical mass spectrum obtained using  $\text{CS}_2$  is presented in the Fig. 2,*a*, which shows the ion current on a logarithmic scale against the selected ion mass. After some optimization, the strongest peak is indeed the parent ion,  $\text{CS}_2^+$ , accompanied with  $^{13}\text{C}$  and  $^{34}\text{S}$  isotopic satellites. Also present is a number of easily identifiable fragments, in particular  $\text{S}_2$ ,  $\text{CS}$ ,  $\text{S}$ , and  $\text{C}$ . Typically the most intense mass peaks from the source corresponded to an ion current of about  $1\text{--}2 \text{ nA}$ .

In Fig. 3 we present an infrared spectrum of a sample resulting from a 3 h deposition of  $1.5 \text{ nA}$  current of ions with mass  $76 \text{ amu}$ . In spite of the nearly a factor of 10 shorter deposition time than in the experiments of Leroi et al, a weak sharp peak at

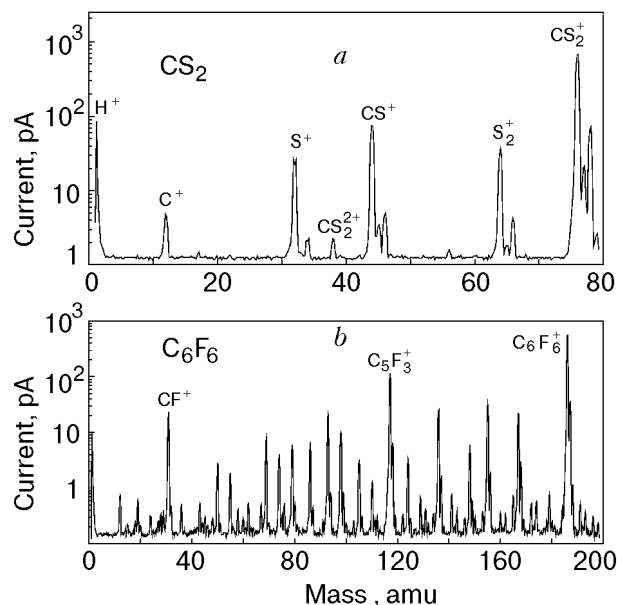


Fig. 2. Mass spectra obtained from our discharge source for the ions investigated in this work:  $\text{CS}_2$  (a) and  $\text{C}_6\text{F}_6$  (b).

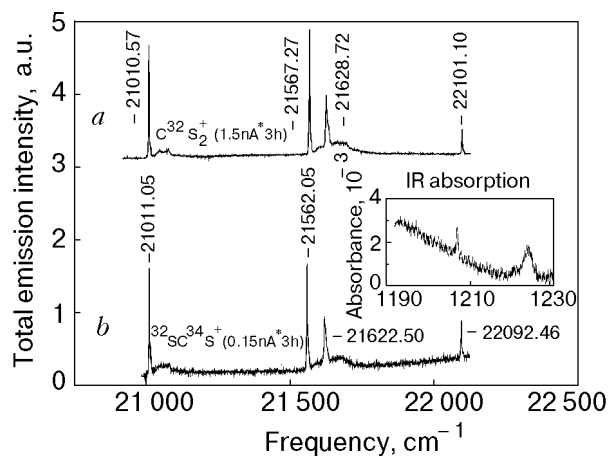


Fig. 3. Partial excitation spectra of the mass selected  $^{12}\text{C}^{32}\text{S}_2^+$  (a) and  $^{34}\text{S}^{12}\text{C}^{32}\text{S}^+$  (b) ions in solid neon matrix. The inset shows the infrared absorption spectrum of the latter ion.

$1206.92 \text{ cm}^{-1}$ , very close to the  $1207.1 \text{ cm}^{-1}$  frequency assigned by them to the  $\nu_3$  asymmetric stretching vibration of  $\text{CS}_2^+$  in solid neon [29], is clearly observable in the spectrum. In contrast with their study, we find in our samples little evidence of either the  $\text{CS}$  fragment at  $1273.7 \text{ cm}^{-1}$ , or of the  $\text{CS}_2^-$  anion at  $1159.4 \text{ cm}^{-1}$ . If present at all, their concentrations relative to that of the  $\text{CS}_2^+$  cation must be at least a factor of ten lower than in the earlier experiments. We have therefore no information as to the identity of the negatively charged species maintaining neutrality of the matrix. The absence of  $\text{CS}$  suggests that dissociative recombination with of the  $\text{CS}_2^+$  cation with electron does not occur to any appreciable extent in our study.

The presence of  $\text{CS}_2^+$  is then unambiguously confirmed by the laser induced fluorescence experiments. Figure 3,*a* shows a total excitation spectrum of the matrix obtained by scanning a laser directed onto the matrix sample over the spectral range near the origin of the well known  $A^2\Pi_u \leftrightarrow X^2\Pi_g$   $\text{CS}_2^+$  transition [47,48]. The spectrum shows clearly the (0,0,0) origin band at  $21010.57 \text{ cm}^{-1}$ , as well as several excited vibrational levels, the (1,0,0), (0,2,0) Fermi resonance doublet at  $21567.27$  and  $21628.72 \text{ cm}^{-1}$ , and the (2,0,0) level at  $22101.0 \text{ cm}^{-1}$ .

The remaining, and most important question which has to be answered is whether the observed  $\text{CS}_2^+$  are really due to the ion deposition, or whether they could be due to neutral  $\text{CS}_2$  from the source reaching the matrix, and being ionized by the electrons from the tungsten filament, or by the ions from the molecular beam. This question is unambiguously resolved by the Fig. 3,*b* from a separate experiment, where the mass filter was tuned to mass 78 rather than 76, and ions of  $0.15 \text{ nA}$  current were

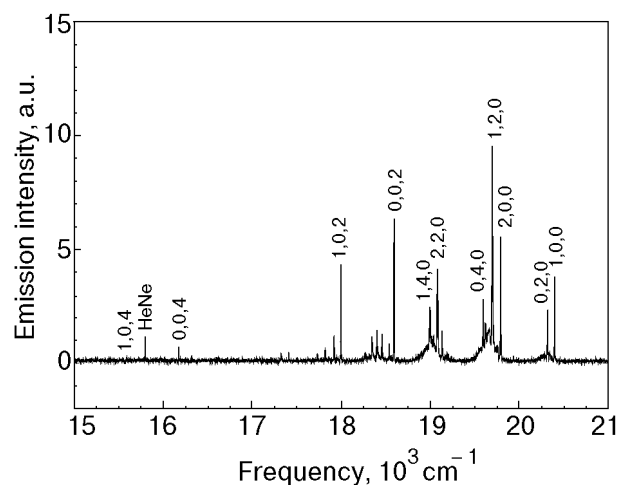


Fig. 4. Laser induced fluorescence spectrum of the mass selected  $^{12}\text{C}^{32}\text{S}_2^+$  molecular ion excited at  $21567\text{ cm}^{-1}$  (1,0,0).

deposited again over 3 hours. One obtains a spectrum very similar to Fig. 3,a, but with the bands distinctly shifted to  $21011.05$ ,  $21562.05$ ,  $21622.50$ , and  $22092.46\text{ cm}^{-1}$ . These are clearly attributable to the  $^{34}\text{S}^{12}\text{C}^{32}\text{S}^+$  molecular ion present in a natural isotopic abundance in our sample.

A resolved fluorescence spectrum of  $\text{CS}_2^+$  is shown in Fig. 4, and a similar spectrum was also recorded for the isotopic  $^{34}\text{S}^{12}\text{C}^{32}\text{S}^+$  cation, with the observed bands and their assignments listed in the Table 1. The measured frequencies are in general in good agreement with previous studies, but in view of the higher signal to noise in the present work, a number of new bands was detected. The most prominent features in the emission spectrum are «Fermi polyads» due to the near resonance between  $\nu_1$  and  $2\nu_2$ . While the assignments of the first two polyads, that is the resonant (1,0,0), (0,2,0) levels and the levels involving the  $2\nu_1$  overtone: (2,0,0), (1,2,0), (0,4,0) are quite unambiguous, for the higher overtones the spectra become more complex, and more levels are detected than expected. Some of this complexity probably arises from the Renner–Teller splitting in the degenerate  $X^2\Pi_g$  state, or is caused by additional resonances involving the  $\nu_3$  asymmetric stretching mode.

A strong band at  $18592.98\text{ cm}^{-1}$  is clearly the overtone of the asymmetric stretching vibration, yielding a value of  $2\nu_3'' = 2417.75\text{ cm}^{-1}$ . This band is again origin of a series of polyads due to combinations with  $\nu_1''$  and  $2\nu_2''$ . Combining the  $2\nu_3$  value from the electronic spectrum with the infrared fundamental  $\nu_3'' = 1206.92\text{ cm}^{-1}$  gives  $x_{3,3}'' = -1.955\text{ cm}^{-1}$ . Such negative anharmonicity is quite common for asymmetric vibrations of symmet-

ric molecules which often have a partial quartic oscillator character, since odd terms are not possible in the potential energy expansion. Similar but even larger negative anharmonicity was also found in the

Table 1

Observed bands of mass selected  $\text{CS}_2^+$  in solid neon (all values in  $\text{cm}^{-1}$ )

$(\nu_1, \nu_2, \nu_3)$	$^{32}\text{S}^{13}\text{C}^{32}\text{S}^+$	$^{32}\text{S}^{12}\text{C}^{32}\text{S}^+$	$^{32}\text{S}^{12}\text{C}^{32}\text{S}^+$	$^{34}\text{S}^{12}\text{C}^{32}\text{S}^+$
	from Ref. 48		this work	
(2,0,0)	22063	22114	22101.1	22092.5
(0,2,0)	21601	21639	21628.7	21622.5
(1,0,0)	21541	21578	21567.3	21562.0
(0,0,0)	21011	21016	21010.6	21011.0
(1,0,0)	20402	20398	20392.9	20398.5
(0,2,0)	20325	20318	20312.9	20317.4
?			19935.7	
(2,0,0)	19809	19792	19788.3	19797.4
(1,2,0)	19710	19700	19695.6	19710.1
(0,4,0)	19627	19600	19595.4	19604.2
(3,0,0)	19218	19188	19202.1?	19197.2?
(2,2,0)	19101	19082	19076.6	19094.3
(1,4,0)	19019	18996	18992.7	19009.0
(0,6,0)?	18912		18863.0	
(0,0,2)	18671	18598	18592.8	18598.6
(1,0,2)	18080		17994.2	18006.0
(0,0,4)			16170.3	
(1,0,4)			15589.7	

excited  $\text{CS}_2^+$   $A^2\Pi_u$  state. Using this anharmonic term, one can predict the next overtones to be  $3\nu_3'' \approx 3632.49$  and  $4\nu_3'' \approx 4851.14\text{ cm}^{-1}$ . While the third overtone should, just like the fundamental, be inactive, a strong band is observed at  $16170.34\text{ cm}^{-1}$ , close to  $16159.43\text{ cm}^{-1}$  where the emission into the (0,0,4) level is predicted.

In Table 1 we also list the frequencies measured for the isotopic  $^{34}\text{S}^{12}\text{C}^{32}\text{S}^+$  ion. In the previous studies both normal  $^{12}\text{C}^{32}\text{S}_2^+$  as well as the isotopic  $^{13}\text{C}^{32}\text{S}_2^+$  ions were investigated [47,48]. Based on the isotopic shifts it was concluded that in both

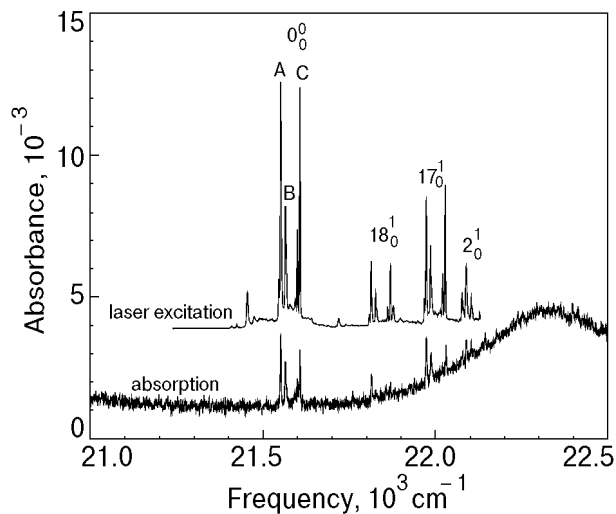


Fig. 5. Laser excitation (top) and absorption (bottom) spectrum of the hexafluorobenzene radical cation,  $C_6F_6^+$ . Note besides the bands due to the main site A also the presence of several additional, spectrally shifted sites.

electronic states involved in the transition the  $\nu_1$  and  $2\nu_2$  levels are almost perfectly mixed. While one would expect the symmetric stretching vibration  $\nu_1$  to exhibit no  $^{13}C$  isotopic shift,  $\rho \approx 1.0$ , while for  $\nu_2$  an isotopic parameter  $\rho \approx 1.034$  can be predicted, both  $\nu_1$  and  $2\nu_2$  exhibited almost identical shifts just in the middle between these two values. Basically the same conclusion can be made in the present work based on the observed  $^{34}S$  isotopic shifts. Strictly speaking,  $^{34}S^{12}C^{32}S^+$  is no longer a symmetric  $D_{\infty h}$  molecule, and therefore also the odd overtones, for instance the  $\nu_3$  and  $3\nu_3$  levels could in principle appear directly in the spectrum. Unfortunately, due to the relatively low isotopic abundance of  $^{34}S$  the spectra of the mixed isotopomer exhibit a somewhat lower signal to noise ratio, and these levels were not detected.

Another previously well known ion which we have now investigated with our new experimental apparatus is  $C_6F_6^+$ , the hexafluorobenzene cation. It is known that it possesses a fully allowed  $\pi-\pi^*$  transition in the visible, and is known to fluoresce in matrices with close to unity quantum yield [49]. To produce the ion, we have again employed a microwave discharge through a pure parent  $C_6F_6$  at a pressure of about  $10^{-3}$  mTorr. One of the problems of such approach is the extensive fragmentation of the parent, resulting in a very complex mass spectrum. As shown in Fig. 2, *b* after optimization the parent ion is the strongest peak in the spectrum, but a large number of fragments and other reaction products is observed, with just about any  $C_nF_m$  ion with  $n$  and  $m$  ranging up to at least 8 being present.

In Fig. 5 we compare an absorption spectrum of a sample resulting from 4 h deposition with the mass filter set to 186 amu with the corresponding excitation spectrum. This was obtained by monitoring the intensity of the sample fluorescence, and scanning the exciting laser in this spectral region. A very strong emission clearly attributable to  $C_6F_6^+$  is indeed observed, but both the absorption and laser excitation spectra exhibit some interesting differences when compared with the previous studies, where the cation was produced by in-situ 1216 Å Lyman  $\alpha$  vacuum UV radiation photoionization of the parent hexafluorobenzene. While the photoionized spectra exhibited essentially a single site and a narrow inhomogeneous distribution, the ion-beam deposited samples contain, besides the «major»  $C_6F_6^+$  site A with origin at  $21551.77\text{ cm}^{-1}$ , numerous other sites, which exhibit appreciable spectral shifts, both to higher and lower energies.

Some time ago we have similarly compared spectra of several ionic species prepared in our laboratory by in situ photolysis of the parent neutrals in neon matrices, with the corresponding species deposited by Maier and coworkers from mass selected ion beams [32,33]. While the ionization produced matrices yielding well defined, sharp lines, the ion beam deposition resulted in broad, structured bands with widths exceeding  $150\text{ cm}^{-1}$ . We have at that time explained this difference by inhomogeneous broadening, due to damage to the neon matrix caused by the impact of the energetic,  $\approx 60\text{ eV}$  ions. The present investigation seems to confirm this interpretation. While the in situ photolysis produces a single site with origin at  $21551.77\text{ cm}^{-1}$ , even though in our case the energy of the ions is believed to be  $\leq 20\text{ eV}$ , their deposition results in about a dozen discrete sites, whose origins span a range of more than  $200\text{ cm}^{-1}$ , from  $21409.43$  to  $21640.44\text{ cm}^{-1}$ . In one experiment, on the other hand, where the energy of the deposited ions was lowered, the subsidiary sites almost disappeared, and the «main» site which was observed and investigated in the previous studies was dominant.

In Table 2 we list the observed transitions of  $C_6F_6^+$  both for the «main» site A, as well as for the two strongest «new» sites B and C, which are blue shifted by  $12.9$  and  $55.3\text{ cm}^{-1}$ , respectively. In Fig. 6, a comparison of the spectra and frequencies of the «main» site A with those of the new sites B and C reveals, that while the progression in the totally symmetric mode,  $\nu_2$ , is essentially identical for the three sites, and also identical with the known gas phase frequencies, the other levels involving the Jahn–Teller active modes  $\nu_{18}$  and

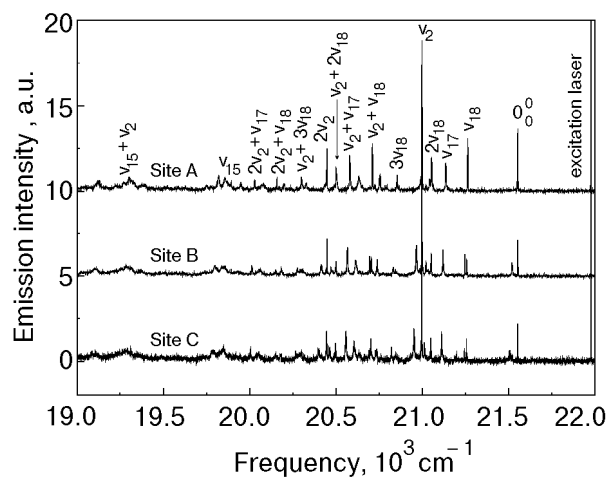


Fig. 6. Comparison of the LIF spectrum of the main site A with those of two of the «perturbed» sites, denoted B and C. For ease of comparison, the spectra of these sites were shifted to make the 0–0 origins overlap. Note the splitting of the spectral lines, as well as the presence of broader satellite bands near the 0–0 origin and other totally symmetric bands.

$\nu_{17}$  [50] exhibit strong perturbations. Thus the  $288.8 \text{ cm}^{-1}$   $\nu_{18}$  level, is in both of the strongest perturbed sites split into two components, both of them blue shifted to about  $295$  and  $305 \text{ cm}^{-1}$ , respectively. Similarly,  $\nu_{17}$  which occurs at  $417.2 \text{ cm}^{-1}$  in the main site is shifted to  $432.8$  and  $440.9 \text{ cm}^{-1}$  in the two other sites. This applies also to their combination and overtone bands. In general, the vibrational levels involving the Jahn–Teller active modes are in all the new sites strongly shifted and sometimes split in several components, and new absorptions appear. Also the 0–0 band, and each of the bands of the strong, totally symmetric  $\nu_2$  progression which is seen up to  $\nu_2 = 3$ , exhibit in the spectra of the new sites a broader satellite band, shifted in emission by  $\approx 33$  and  $46 \text{ cm}^{-1}$ , respectively.

Table 2

Observed bands of mass selected  $\text{C}_6\text{F}_6^+$  in solid neon («main» site A and perturbed sites B and C, all values in  $\text{cm}^{-1}$ )

Mode	from Ref. 49	A	B	C
$\nu_2'$	540	537.4	537.5	
$\nu_{17}'$	426	422.5	420.8	424.0
$\nu_{18}'$	265	263.9	263.2	263.5
0–0 $X_1$	21558	21551.8	21565.3	21607.0
0–0 $X_2$			32.8	46.1
$\nu_{18}$	289	288.8	294.7	296.9

$\nu_{18a}$			305.0	308.3
$\nu_{17}$	417	417.2	432.8	440.9
$\nu_{17} + \nu_{18}$	498	497.9	500.9	503.0
$2\nu_{18}$	508	508.8	528.6	541.1
		529.9	567.2	
$\nu_2$	554	553.1	553.6	554.7
		560.3	560.4	560.5
$\nu_2 X_2$			585.5	599.1
			710.2	707.6
$3\nu_{18}$	699	698.5	721.9	731.4
	759	758.4		
	770	770.0		
$2\nu_{17}$	797	797.3	814.7	816.2
		801.2		823.8
	826	825.9		
		830.1		
$\nu_2 + \nu_{18}$	843	842.6	848.9	851.9
$\nu_2 + \nu_{18a}$			859.0	862.7
$4\nu_{18}$	919	919.3		
$\nu_2 + \nu_{17}$	972	971.2	986.8	995.4
$\nu_2 + 2\nu_{18}$	1052	1052.0		
$2\nu_2$	1107	1106.5	1107.0	1108.5
$2\nu_2 X_2$			1141.0	1153.1
$\nu_{16}$	1226	1225.0	1246.5	
$\nu_2 + 3\nu_{18}$	1253	1252.2	1274.8	1286.2
	1280	1278.8		
		1310.1		
$\nu_2 + \nu_{17} + 2\nu_{18}$ (?)	1324			
$\nu_2 + 2\nu_{17}$	1352	1350.7		
$2\nu_2 + \nu_{18}$	1397	1396.0	1402.3	
$2\nu_2 + \nu_{18a}$			1412.5	
$\nu_2 + 4\nu_{18}$	1474	1473.3		
$2\nu_2 + \nu_{17}$	1526	1524.9		
$2\nu_2 + 2\nu_{18}$	1605	1604.6		
$3\nu_2$	1661	1659.6	1660.2	?
	1682	1681.4		
$\nu_{15}$	1698	1694.1	1696.2	1706.6
	1734	1732.9		
	1805	1805.2		
		1966.5		
	2172	2165.2		
	2220	2219.9		
$\nu_{15} + \nu_2$	2250	2248.9		
		2281.6		
	2432			

A tentative interpretation of these observations is that when produced by in situ photolysis of the parent, the  $\text{C}_6\text{F}_6^+$  cation is in an unperturbed site with relatively high symmetry. When, however, the ion is deposited in the matrix from the gas phase with kinetic energies of  $\approx 20 \text{ eV}$ , lower symmetry

sites, perhaps with nearby vacancies, are produced and populated, which strongly affect the Jahn–Teller distortion, perturb the related vibrational structure, and relax the selection rules. An interesting question involving the doubly degenerate ground state of  $C_6F_6^+$  and similar cations is the magnitude of the spin orbit splitting. Several older theoretical works suggested that this is probably small [51], but there is little a priori evidence on this point. Compared with the spin orbit constants in a number of small compounds of first row elements, the observed 33–46  $cm^{-1}$  separation of the two components of the origin band, as well as of the other totally symmetric levels would seem to be of the right order of magnitude to be assigned to the spin-orbit splitting of the degenerate  $X^2E_{1g}$  ground state of the  $C_6F_6^+$  cation.

If one accepts this assignment, then considering that the magnitude of the splitting changes by some 30% between the two sites examined, the question arises as to how much of this is intrinsic, free  $C_6F_6^+$  splitting, and how much is due to the asymmetric environment. In other words, one might ask if one sees an extra component because the selection rules are relaxed, and a level which is not accessible in a symmetric site becomes visible when the site symmetry is lowered, or because the initially degenerate and unresolvable levels were split by the asymmetry. An unambiguous answer to these question will require additional study. It should be noted, that the spin orbit splitting was neglected in most previous treatments of the substituted benzene cations. Strictly speaking, however, the spin–orbit and Jahn–Teller interactions are not independent of each other, and if both splittings are non-negligible, both would have to be simultaneously considered in a rigorous treatment of the  $X^2E_{1g}$  ground state vibrational structure.

### Conclusion

In the present manuscript we present preliminary results obtained with a new apparatus for deposition of mass selected ions in low temperature matrices. With this apparatus we obtain infrared and visible absorption, as well as fluorescence and fluorescence excitation spectra of mass selected ions. We demonstrate the successful and clean mass selection by presenting spectra of samples obtained by depositing the isotopic  $^{34}S^{12}C^{32}S^+$  ion in natural isotopic abundance. Experiments with  $C_6F_6^+$  demonstrate, that deposition of ions with high kinetic energy from the gas phase, produces quite different inhomogeneous line profile, and results in a variety of «perturbed» sites, presumably due to nearby

defects and vacancies. The emission spectra of the perturbed sites are characterized by appreciable shifts and doubling of the vibrational levels of the degenerate  $X^2E_{1g}$  ground state, which may be due to combination of the spin orbit splitting and the Jahn–Teller effect.

### Acknowledgement

We gratefully acknowledge the Deutsche Forschungsgemeinschaft which contributed essentially to funding this project, as well as the Fond der Chemischen Industrie for generous support.

1. E. Whittle, D. A. Dows, and G. C. Pimentel, *J. Chem. Phys.* **22**, 1943 (1954).
2. V. E. Bondybey, A. M. Smith, and J. Agreiter, *Chem. Rev.* **96**, 2113 (1996).
3. M. S. Sabo, J. Allison, J. R. Gilbert, and G. E. Leroi, *Appl. Spectrosc.* **45**, 535 (1991).
4. J. P. Maier, *Mass Spectrometry Rev.* **11**, 119 (1992).
5. S. Fedrigo, F. Meyer, D. M. Lindsay, J. Lignieres, J. C. Rivoal, and D. Kreisle, *J. Chem. Phys.* **93**, 8535 (1990).
6. T. M. Halasinski, J. T. Godbout, J. Allison, and G. E. Leroi, *J. Phys. Chem.* **100**, 14865 (1996).
7. P. Fayet and L. Wöste, *Z. Phys.* **D3**, 177 (1986).
8. J. C. Rivoal, C. Grisolia, J. Lignieres, D. Kreisle, P. Fayet, and L. Wöste, *Z. Phys.* **D12**, 481 (1989).
9. S. Fedrigo, W. Harbich, and J. Buttet, *J. Chem. Phys.* **99**, 5712 (1993).
10. W. Harbich, S. Fedrigo, and J. Buttet, *Z. Phys.* **D26**, 138 (1993).
11. W. Harbich, Y. Belyaev, R. Kleiber, and J. Buttet, *Surf. Rev. Lett.* **3**, 1147 (1996).
12. Z. Hu, B. Shen, Q. Zhou, S. Deosaran, J. R. Lombardi, D. M. Lindsay, and W. Harbich, *J. Chem. Phys.* **95**, 2206 (1991).
13. Z. Hu, G. Jian, J. R. Lombardi, and D. M. Lindsay, *J. Chem. Phys.* **97**, 8811 (1992).
14. Z. Hu, B. Shen, J. R. Lombardi, and D. M. Lindsay, *J. Chem. Phys.* **96**, 8757 (1992).
15. Z. Hu, G. Jian, J. R. Lombardi, and D. M. Lindsay, *J. Phys. Chem.* **97**, 9263 (1993).
16. Z. Hu, G. Jian, J. R. Lombardi, and D. M. Lindsay, *J. Chem. Phys.* **101**, 95 (1994).
17. J. Dong, Z. Hu, R. Craig, J. R. Lombardi, and D. M. Lindsay, *J. Chem. Phys.* **101**, 9280 (1994).
18. H. Haouari, H. Wang, R. Craig, J. R. Lombardi, and D. M. Lindsay, *J. Chem. Phys.* **103**, 9527 (1995).
19. H. Wang, R. Craig, H. Haouari, J. Dong, Z. Hu, A. Vivoni, J. R. Lombardi, and D. M. Lindsay, *J. Chem. Phys.* **103**, 3289 (1995).
20. H. Wang, H. Haouari, R. Craig, J. R. Lombardi, and D. M. Lindsay, *J. Chem. Phys.* **104**, 3420 (1996).
21. H. Wang, R. Craig, H. Haouari, Y. Liu, J. R. Lombardi, and D. M. Lindsay, *J. Chem. Phys.* **105**, 5355 (1996).
22. H. Wang, H. Haouari, R. Craig, Y. Liu, J. R. Lombardi, and D. M. Lindsay, *J. Chem. Phys.* **106**, 2101 (1997).
23. H. Wang, Y. Liu, H. Haouari, R. Craig, J. R. Lombardi, and D. M. Lindsay, *J. Chem. Phys.* **106**, 6534 (1997).
24. H. Wang, Z. Hu, H. Haouari, R. Craig, Y. Liu, J. R. Lombardi, and D. M. Lindsay, *J. Chem. Phys.* **106**, 8339 (1997).



25. H. Wang, Y. Liu, H. Haouari, R. Craig, J. R. Lombardi, and D. M. Lindsay, *J. Phys. Chem.* **A101**, 7036 (1997).
26. J. R. Gilbert, G. E. Leroi, and J. Allison, *Int. J. Mass Spectr. Ion Proc.* **107**, 247 (1991).
27. J. T. Godbout, T. M. Halasinski, G. E. Leroi, and J. Allison, *J. Phys. Chem.* **100**, 2892 (1996).
28. T. M. Halasinski, J. T. Godbout, G. E. Leroi, and J. Allison, *J. Phys. Chem.* **98**, 3930 (1994).
29. T. M. Halasinski, J. T. Godbout, J. Allison, and G. E. Leroi, *J. Phys. Chem.* **100**, 14865 (1996).
30. D. Forney, M. Jakobi, and J. P. Maier, *J. Chem. Phys.* **90**, 600 (1989).
31. J. P. Maier, *Chem. Soc.* **26**, 21 (1997).
32. P. Freivogel, J. Fulara, D. Lessen, D. Forney, and J. P. Maier, *Chem. Phys.* **189**, 335 (1994).
33. J. Fulara, P. Freivogel, D. Forney, and J. P. Maier, *J. Chem. Phys.* **103**, 8805 (1995).
34. D. Forney, P. Freivogel, J. Fulara, and J. P. Maier, *J. Chem. Phys.* **102**, 1510 (1995).
35. J. Agreiter, A. M. Smith, and V. E. Bondybey, *Chem. Phys. Lett.* **241**, 317 (1995).
36. A. M. Smith, J. Agreiter, and V. E. Bondybey, *Chem. Phys. Lett.* **244**, 379 (1995).
37. M. Grutter, M. Wyss, J. Fulara, and J. P. Maier, *J. Phys. Chem.* **A102**, 9785 (1998).
38. M. Grutter, M. Wyss, and J. P. Maier, *J. Chem. Phys.* **110**, 1492 (1999).
39. P. Freivogel, M. Grutter, D. Forney, and J. P. Maier, *J. Chem. Phys.* **107**, 4468 (1997).
40. M. Tulej, D. A. Kirkwood, G. Maccaferri, O. Dopfer, and J. P. Maier, *Chem. Phys.* **228**, 293 (1998).
41. M. Grutter, M. Wyss, E. Riaplov, and J. P. Maier, *J. Chem. Phys.* **111**, 7397 (1999).
42. M. Tulej, D. A. Kirkwood, M. Pachkov, and J. P. Maier, *Astrophys. J.* **506**, 69 (1998).
43. D. A. Kirkwood, H. Linnartz, M. Grutter, O. Dopfer, C. Motylewski, M. Pachkov, M. Tulej, M. Wyss, and J. P. Maier, *Faraday Discuss.* **109**, 109 (1998).
44. S. Fedrigo, T. L. Haslett, and M. Moskovits, *J. Am. Chem. Soc.* **118**, 5083 (1996).
45. T. L. Haslett, K. A. Bosnick, and M. Moskovits, *J. Chem. Phys.* **108**, 3453 (1998).
46. T. L. Haslett, K. A. Bosnick, S. Fedrigo, and M. Moskovits, *J. Chem. Phys.* **111**, 6456 (1999).
47. V. E. Bondybey, J. H. English, and T. A. Miller, *J. Chem. Phys.* **70**, 1621 (1979).
48. V. E. Bondybey, J. H. English, *J. Chem. Phys.* **73**, 3098 (1980).
49. V. E. Bondybey and T. A. Miller, *J. Chem. Phys.* **73**, 3035 (1980).
50. T. J. Sears, T. A. Miller, and V. E. Bondybey, *J. Chem. Phys.* **74**, 3240 (1981).
51. H. M. McConnel, *J. Chem. Phys.* **34**, 13 (1961).